

## Influence of Cd<sup>2+</sup> Ions Substitution on the Magnetic Properties of Ni-Cd Ferrites

V.S. Bushkova\*

Vasyl Stefanyk Precarpathian National University, 57, Shevchenko St., 76025 Ivano-Frankivsk, Ukraine

(Received 03 July 2017; revised manuscript received 10 July 2017; published online 16 October 2017)

The polycrystalline of Ni-Cd ferrites were prepared by the technology sol-gel with participation of auto-combustion and sintered at temperature 1573 K in air. Low field hysteresis measurement was carried out at room temperature at frequency of 200 Hz and at the field range 1600-16000 A/m. The increase of Cd<sup>2+</sup> ions yields the increase of specific saturation magnetization  $\sigma_s$  and magnetic moment  $m_{exp}$  up to  $x = 0.3$  then decrease thereafter. The Neel's two sublattice model can be applied to the sample up to  $x = 0.3$ . The composition dependence of the specific saturation magnetization and magnetic moment for  $0.4 \leq x \leq 0.6$  were explained on the basis of the existence of Yafet-Kittel angles on the B-site spins. The temperature variation of the initial permeability  $\mu_i$  of these samples was carried out from 300 to 900 K. The initial permeability increases with increasing Cd content up to  $x = 0.3$  after that it decreases. It was found that Curie temperature  $T_c$  decreases from 831 to 697 K.

**Keywords:** Ferrites, Specific saturation magnetization, Magnetic moment, Initial permeability, Curie temperature.

DOI: 10.21272/jnep.9(5).05029

PACS numbers: 75.75.+a, 75.60.-d

### 1. INTRODUCTION

Ferrites are used in various technological applications due to their high electrical resistivity and wide range of saturation magnetization [1, 2]. Nickel ferrite NiFe<sub>2</sub>O<sub>4</sub> in pure and substituted form constitutes technologically important materials, which have been studied in many experimental and theoretical works [3]. Cadmium ferrite CdFe<sub>2</sub>O<sub>4</sub> is well known as one type of the geometrically frustrated systems [4]. According to literature report [5] cadmium ions occupy tetrahedral A-site. The substitution of Cd<sup>2+</sup> in ferrite is well-known to enhance the magnetic properties like saturation magnetization [6].

Ni-Cd spinel ferrite synthesized by ceramic technique in bulk form has been investigated by many workers [7]. There are many methods for preparation of nanoparticle ferrites [8]. Also for reduction in the grain size of polycrystalline ferrites new methods such as hydrothermal synthesis [9], chemical co-precipitation [10], sol-gel methods [11] are used to form a fine-grained ceramic. The properties of nanoparticles are interesting due to the presence of very highly disordered grain boundaries. The geometrically frustrated antiferromagnets are distinguishable from other magnetic systems in a number of exceptional features as their formation, to a great extent, depends on the range as well as the nature of the interactions between the magnetic ions in the systems [12].

The aim of present work is study the role of Cd<sup>2+</sup> ions substitution at tetrahedral A-site by replacing Ni<sup>2+</sup> ions and their effect on magnetic properties of NiFe<sub>2</sub>O<sub>4</sub> prepared by the technology sol-gel with participation of auto-combustion (SGA).

### 2. EXPERIMENTS

Cadmium substituted ferrites with the general formula Ni<sub>1-x</sub>Cd<sub>x</sub>Fe<sub>2</sub>O<sub>4</sub> ( $x = 0.0, 0.1, 0.2, 0.3, 0.4, 0.5$  and  $0.6$ ) have been prepared by SGA technique. The detailed

process is described as follows: citric acid (C<sub>6</sub>H<sub>8</sub>O<sub>7</sub> · H<sub>2</sub>O), ferric nitrate (Fe(NO<sub>3</sub>)<sub>3</sub> · 9H<sub>2</sub>O), nickel nitrate (Ni(NO<sub>3</sub>)<sub>2</sub> · 6H<sub>2</sub>O) and cadmium nitrate (Cd(NO<sub>3</sub>)<sub>2</sub> · 4H<sub>2</sub>O) were used as starting materials. The molar ratio of metal nitrates to citric acid was taken as 1:1. The metal nitrates were dissolved together in 50 ml of distilled water to get a clear solution. An aqueous solution of citric acid was mixed with metal nitrates solution. Then ammonia solution was slowly added to adjust the pH at 7. The mixed solution was dried at a temperature around 403 K. During evaporation the solution become viscous and finally formed a xerogel (Fig. 1). After several minutes the xerogel automatically ignited. The decomposition reaction would not stop before the whole citrate complex was consumed. The auto-combustion was completed within a minute, yielding the nanopowders (Fig. 2).



Fig. 1 – The dried gel of NiFe<sub>2</sub>O<sub>4</sub> sample

The X-ray diffraction (XRD) patterns were recorded at room temperature on Dron 3 X-ray diffractometer using CuK $\alpha$  ( $\lambda = 0.15418$  nm) radiation. The scanning was done in the  $2\theta$  range from 15° to 60°. After completing the process auto-combustion was obtained one phase of NiFe<sub>2</sub>O<sub>4</sub> powder which corresponded to the cubic structure of spinel space group *Fd3m*. Ferrite powders, replaced by nonmagnetic ions, were contained additional phases oxides NiO, CdO and  $\alpha$ -Fe<sub>2</sub>O<sub>3</sub>. After annealing at a temperature of 1173 K for 3 hours was received monophasic powders. The average size of coherent scattering regions of monophasic powders was in the range 42-61 nm [13].

\* bushkovavira@gmail.com



**Fig. 2** – Appearance of nickel powder

The formed core of ferrite powders in the form of a thoroid was subjected to annealing at a temperature of 1573 K for 5 hours in an atmosphere of air with slow cooling. The measurement of the inductance  $L$  of the coils was carried out at a frequency of 1 kHz using a digital LCR meter E7-8 in a weak magnetic field in the temperature range of 293-873 K. The investigation of the magnetic properties of the samples was carried out by constructing magnetic hysteresis loops obtained with the help of an electronic digital ferrometer F-5064 at a frequency of 200 Hz.

### 3. RESULTS AND DISCUSSION

#### 3.1 Magnetic Studies

The compounds of the system  $\text{Ni}_{1-x}\text{Cd}_x\text{Fe}_2\text{O}_4$  showed a definite hysteresis loop at room temperature, which indicates the ferrimagnetic behaviour (Fig. 3). From the hysteresis loops, the coercive force  $H_c$  and specific saturation magnetization  $\sigma_s$  have been calculated and are listed in Table 1. From Table 1 it is seen that the specific saturation magnetization increases with increase in cadmium content upto  $x = 0.3$  and shows decreasing trend later on. This is due to the fact that cadmium ions have the preference for tetrahedral  $A$  sites, nickel ions for octahedral  $B$  sites and iron ions are distributed among octahedral and tetrahedral sites. The cation distribution is given by

$$\left(\text{Cd}_x^{2+}\text{Fe}_{1-x}^{3+}\right)\left[\text{Ni}_{1-x}^{2+}\text{Fe}_{1+x}^{3+}\right]_4^{2-}, \quad (1)$$

where the ions enclosed by round brackets correspond to tetrahedral or  $A$ -site and the ions enclosed by square brackets corresponds to octahedral or  $B$ -site.

According to the Neel's model the resultant magnetization is the difference between  $A$ -site and  $B$ -site magnetization, provided that they are collinear and anti-parallel to each other. Mathematically,

$$m_{th} = m(B) - m(A). \quad (2)$$

The substitutions of non-magnetic divalent cadmium ions on the  $A$ -sites transfer the trivalent iron ions on  $B$  sites affecting the magnetic moments of individual sub lattice and  $A$ - $B$  interactions. As the cadmium

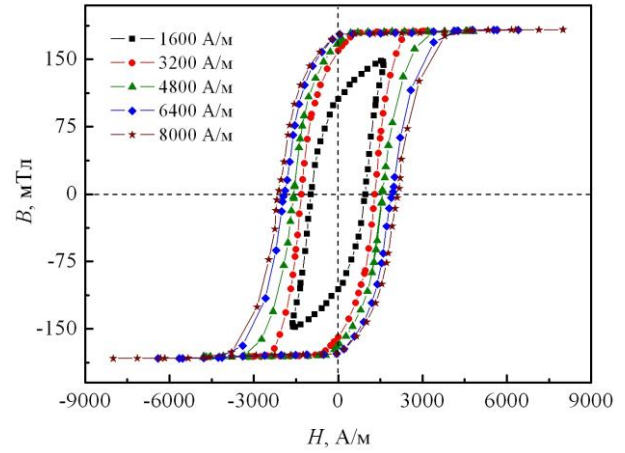


**Fig. 3** – Magnetization curve of  $\text{NiFe}_2\text{O}_4$  ferrite as field function

ions increase at  $A$  site, the magnetization of tetrahedral site decreases, this results in an increase of net magnetization, which is in agreement with Neel's model.

With further increase in cadmium concentration Neel's two sublattice model is unable to explain the decrease of magnetization beyond  $x = 0.3$  at room temperature. The decrease of magnetization can be treated theoretically by triangular arrangement of spins as proposed by Yafet and Kittel. Therefore, in the present system the concentration dependence of  $\sigma_s$  can be attributed to canting of spins which gives rise to Yafet-Kittel (Y-K) angles, suggesting  $A$ - $B$  and  $B$ - $B$  super exchange interactions to be comparable in strength. Y-K angles are computed from the data obtained in the hysteresis experiment using following equation:

$$\cos \alpha_{Y-K} = \frac{m_{exp} + 5 \cdot (1-x)}{7+x}, \quad (3)$$

where  $m_{exp}$  is expressed in the units of Bohr-magneton and  $x$  represents the contents of cadmium.

The Y-K angles are found to increase with the increase of Cd-content (Table 1). The physical origin of this spin arrangement is from the canting of the spins in the  $B$ -sublattice due to weakening of the intersublattice interaction  $J_{AB}$  and enhancing of intersublattice interaction  $J_{BB}$  on nonmagnetic  $\text{Cd}^{2+}$  substitution in the  $A$ -sublattice. As in the case of spinels,  $J_{BB}$  is antiferromagnetic, the  $B$ -sublattice splits into two sublattices forming Y-K angle between the directions of the spins resulting in a decrease of net  $B$ -sublattice magnetization. If the spin canting has not

**Table 1** – Magnetic properties and average crystallite size ( $T = 1573$  K) for  $\text{Ni}_{1-x}\text{Cd}_x\text{Fe}_2\text{O}_4$  system

$x$	$\langle D \rangle$ , nm	$H_c$ , A/m	$\sigma_s$ , $\text{A} \cdot \text{m} \cdot \text{kg}^{-1}$	$\alpha_{Y-K}$ , $^\circ$
0.0	82	2100	33.9	24° 12'
0.1	93	2310	43.1	27° 12'
0.2	88	2778	52.9	29° 11'
0.3	103	3819	60.9	32° 18'
0.4	81	2068	54.8	43° 46'
0.5	76	2017	38.0	56° 39'
0.6	49	1890	27.7	65° 49'

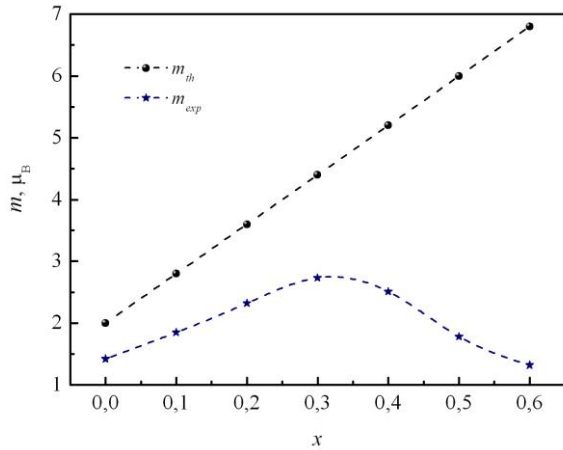


**Fig. 4** – Magnetic moment of  $\text{Ni}_{1-x}\text{Cd}_x\text{Fe}_2\text{O}_4$  as a function of Cd-content

occurred with higher Cd-content, the magnetic moment of the entire series would increase monotonically reaching a value of  $10 \mu_B$  for  $\text{CdFe}_2\text{O}_4$  [14].

The observed magnetic moment dependence on Cd concentration is depicted in Fig. 4, which supports the above argument that Bohr magneton values initially increase with increasing Cd content, supporting Neel’s two sublattice model, reaches to maximum and then decrease at  $x=0.3$ , suggesting change of spin and prevalence of the canted spin arrangement effect in this compound after Cd content. It was detected that the observed magnetic moments for samples with  $x \leq 0.3$  are slightly less than the calculated one. This small variation may be due to the preparation technique.

**3.2 Initial Magnetic Permeability Measurements**

The magnetic initial permeability  $\mu$  for the material is expected to strongly depend on the microstructure, as the magnetic initial permeability represents the mobility of magnetic domain wall in response to the small applied field. The temperature variation of magnetic initial permeability for Ni-Cd samples is shown in Fig. 5. The  $\mu_i$  versus  $x$  curve of Ni-Cd samples show that  $\mu_i$  increases for  $x \leq 0.3$  and decreases for  $x > 0.3$ .

The temperature dependence of magnetic permeability at frequency of 1 kHz is shown in Fig. 6. The straight-line of  $\mu_i(T)$  graphic dependence are used to determine the Curie temperature  $T_C$ . The study of the temperature variation of initial magnetic permeability curves of  $\text{Ni}_{1-x}\text{Cd}_x\text{Fe}_2\text{O}_4$ , with  $x \leq 0.5$ , compounds show

a typical Hopkinson effect. For these samples  $\mu_i$  increases with increasing temperature giving a peak value and then suddenly drops just before the Curie temperature. This is a characteristic behaviour of sample having a single domain grains. Moreover, these samples are showing sharp decrease  $\mu$  at  $T_C$  indicating that impurity phases are not present in the sample and there is single phase formation. This fact is also evidenced by XRD patterns [13]. The sintered at  $T = 1573 \text{ K}$   $\text{Ni}_{0.4}\text{Cd}_{0.6}\text{Fe}_2\text{O}_4$  sample is not single-phase. The absence of single-phase structure is supported by the fact that Hopkinson’s effect was not observed.

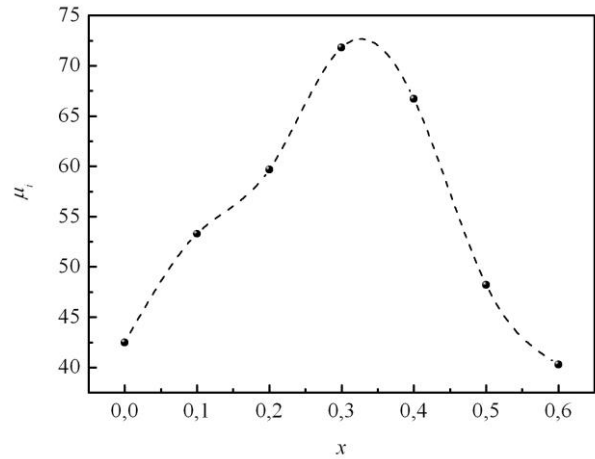


**Fig. 5** – Variation of magnetic permeability with composition  $x$

The experimental Curie temperature  $T_C$  for Ni-Cd compounds is listed in Table 2. It is observed from Table 2 that the  $T_C$  decreased with the  $\text{Cd}^{2+}$  substitutions. The non-magnetic  $\text{Cd}^{2+}$  ions are replacing the  $\text{Ni}^{2+}$  ions having magnetic moment of  $2 \mu_B$ . Therefore, a decrease in the density of magnetic ions is observed and the magnetic moment of the sublattices is expected to decrease. This weakens the  $A-B$  exchange interactions of the Ni-Cd system. Since  $T_C$  is determined by an overall strength of the  $A-B$  exchange interactions, the weakening of the  $\text{Fe}^{3+}(A)-\text{O}^{2-}-\text{Fe}^{3+}(B)$  interaction results in a decrease of the  $T_C$ , when the substitution of  $\text{Cd}^{2+}$  increases in the  $\text{NiFe}_2\text{O}_4$ . The decrease of  $T_C$  can be well correlated with the observed values of Y-K angle in the ferrites.

The theoretical calculation of the Curie temperature for substituted ferrite was obtained by Upadhyay and Baldha model, which instead of considering three magnetic ions per formula unit, considered magnetic moment per formula unit given by equations:

**Table 2** – Curie temperature for  $\text{Ni}_{1-x}\text{Cd}_x\text{Fe}_2\text{O}_4$  system

$x$	$m(x), \mu_B$	$z$	$w$	$n(x), \mu_B$	$T_C(\text{th}), \text{K}$	$T_C(\text{exp}), \text{K}$
0.0	2.40	1.0	1.0	33.60	845	831
0.1	2.36	0.9	1.1	31.54	819	815
0.2	2.32	0.8	1.2	29.18	787	786
0.3	2.28	0.7	1.3	26.54	749	776
0.4	2.24	0.6	1.4	23.62	704	747
0.5	2.20	0.5	1.5	20.40	652	723
0.6	2.16	0.4	1.6	16.90	593	697

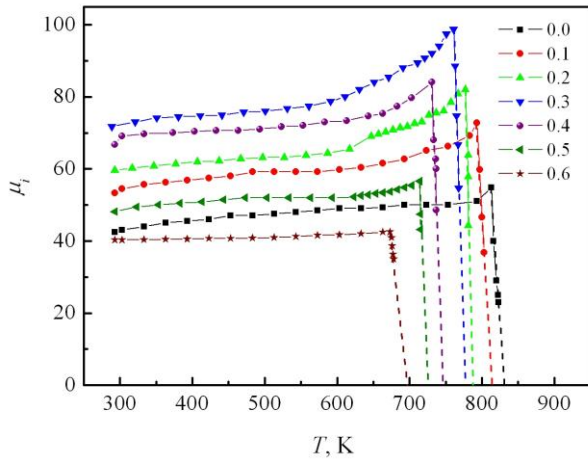


**Fig. 6** – Variation of  $\mu_i$  with temperature for  $\text{Ni}_{1-x}\text{Cd}_x\text{Fe}_2\text{O}_4$  system

$$\overline{m}(x) = 2 + (1-x) \cdot \frac{m(\text{Ni}^{2+})}{m(\text{Fe}^{3+})}, \quad (4)$$

where  $m(\text{Ni}^{2+})$  – the magnetic moment of  $\text{Ni}^{2+}$  ion,  $m(\text{Fe}^{3+})$  – the magnetic moment of  $\text{Fe}^{3+}$  ion,  $x$  – the nonmagnetic ion concentration. The values of magnetic moments of  $\text{Fe}^{3+}$  and  $\text{Ni}^{2+}$  ions used are  $5 \mu_B$  and  $3 \mu_B$  respectively.

The formula for determination of Curie temperature as they put forth is:

$$T_c = \frac{m(x=0) \cdot n(x)}{m(x) \cdot n(x=0)} \cdot T_c(x=0), \quad (5)$$

where  $T_c(x=0)$  is the Curie temperature of unsubstituted ferrite (845 K [15]), and

$$n(x) = \frac{24}{m(\text{Fe}^{3+})} \left[ \frac{z\delta \cdot m^2(\text{Ni}^{2+}) + (\delta w + z^2) \cdot m(\text{Ni}^{2+})}{m(\text{Fe}^{3+}) + wz \cdot m^2(\text{Fe}^{3+})} \right], \quad (6)$$

is the number of relative weighted magnetic interactions per formula unit,

$$z = 1 - x - \delta, \quad (7)$$

$$w = 1 + x + \delta, \quad (8)$$

where  $\delta$  is the fraction of  $\text{Ni}^{2+}$  ions on A site.

Thus the Curie temperature is proportional to the number of active magnetic linkages and can be calculated by using formula:

## Вплив заміщення йонами $\text{Cd}^{2+}$ на магнітні властивості Ni-Cd феритів

В.С. Бушкова

ДВНЗ «Прикарпатський національний університет імені Василя Стефаника»  
вул. Шевченка, 57, 76025 Івано-Франківськ, Україна

Полікристалічні Ni-Cd шпінелі одержано за технологією золь-гель за участі автогоріння та відпалено за температури 1573 K в атмосфері повітря. Вимірювання гістерезису в низьких полях в діапазоні 1600-16000 A/m проведено за кімнатної температури на частоті 200 Гц. Збільшення йонів  $\text{Cd}^{2+}$  призводить до збільшення питомої намагніченості насичення  $\sigma_s$  та магнітного моменту  $m_{exp}$  до  $x = 0,3$ , після чого ці параметри зменшуються. Двох підґраткову модель теорії Нееля можна застосувати до

$$T_c = \frac{m_{\text{NiFe}_2\text{O}_4} \cdot n(x)}{m(x) \cdot n_{\text{NiFe}_2\text{O}_4}}. \quad (9)$$

The Curie temperature calculated theoretically is given in the Table 2. For samples with  $x < 0.3$  the  $T_c$  determined theoretically agrees very well with experimentally determined  $T_c$  indicating the applicability of theoretical model to the present study. The experimental values  $T_c$  are lower than that of reported by Devmunde et al. [16] and are higher than that of reported by Lee et al. [15]. The reduction of Curie temperature in the synthesized nanoparticles is attributed to the existence of a “dead” surface layer for each particle in which magnetic moments do not contribute to the magnetization in the applied field [17]. The lower values of magnetic parameters could be attributed to the fact that surface distortion due to interaction of the transition metal ions with the oxygen atoms in the spinel lattice can reduce the net magnetic moment in the particle.

## 4. CONCLUSION

The  $\text{Ni}_{1-x}\text{Cd}_x\text{Fe}_2\text{O}_4$  ferrites were synthesized by the technology sol-gel with participation of auto-combustion at low temperature. Formation of cubic spinel structure was confirmed by X-ray diffraction analysis.

The occurrence non-collinear spin arrangements results in a sharp decrease of specific saturation magnetization with  $x > 0.3$ . Y-K angle increases on increasing  $\text{Cd}^{2+}$  concentration. The increase in Y-K angles indicate the increasing of favouring of triangular spin arrangement on B-sites leading to an increase in A-B interaction. Thus the observed variation of the magnetization  $\sigma_s$ , which has been explained on the bases of the existence of Yafet-Kittel angles on the B-site spins. The coercive force indicates that the anisotropy character is similar in nature for all samples.

The data on the temperature variation of the initial magnetic susceptibility suggest that these samples have single domain grains. The absence of multi-domain grains is supported by the fact that Hopkinson's effect was observed. The temperature 831 K is required to bring of  $\text{NiFe}_2\text{O}_4$  ferrite in paramagnetic state.  $T_c$  values are found to decrease with increasing  $\text{Cd}^{2+}$  concentration at A-site due to the weakening of A-B interactions.

зразків з  $x \leq 0,3$ . Залежність питомої намагніченості насичення та магнітного моменту при  $0,4 \leq x \leq 0,6$  пояснено на підставі існування кутів Яфета-Кіттеля між спінами В-підґратки. Температурні вимірювання початкової проникності  $\mu_i$  цих зразків проводилися в інтервалі 300-900 К. Початкова проникність збільшується зі збільшенням вмісту Cd до  $x = 0,3$ , після чого  $\mu_i$  зменшується. Виявлено, що температура Кюрі  $T_c$  зменшується від 831 до 697 К.

**Keywords:** Ферити, Питома намагніченість насичення, Магнітний момент, Початкова проникність, Температура Кюрі.

## Влияние замещения ионами Cd<sup>2+</sup> на магнитные свойства Ni-Cd ферритов

В.С. Бушкова

ГВНЗ «Прикарпатский национальный университет имени Василия Стефаника»,  
ул. Шевченко, 57, 76025 Ивано-Франковск, Украина

Поликристаллические Ni-Cd шпинели получено по технологии золь-гель с участием автогорения и отожжено при температуре 1573 К в атмосфере воздуха. Измерение гистерезиса в низких полях 1600-16000 А/м проведено при комнатной температуре на частоте 200 Гц. Увеличение ионов Cd<sup>2+</sup> приводит к увеличению удельной намагнитченности насыщения  $\sigma_s$  и магнитного момента  $m_{exp}$  к  $x = 0,3$ , после чего эти параметры уменьшаются. Двух подрешеточную модель теории Нееля можно применить к образцам из  $x \leq 0,3$ . Зависимость удельной намагнитченности насыщения и магнитного момента при  $0,4 \leq x \leq 0,6$  объяснено на основании существования углов Яфета-Киттеля между спинами В-сайта. Температурные измерения начальной проницаемости  $\mu_i$  этих образцов проводились в интервале 300-900 К. Начальная проницаемость увеличивается с увеличением содержания Cd до  $x = 0,3$ , после чего  $\mu_i$  уменьшается. Обнаружено, что температура Кюри  $T_c$  уменьшается от 831 до 697 К.

**Ключевые слова:** Ферриты, Удельная намагнитченность насыщения, Магнитный момент, Начальная проницаемость, Температура Кюри.

### REFERENCES

1. .K. Kotnala, Jyoti Shah, Bhikham Singh, Hari Kishan, Sukhvir Singh, S.K. Dhawan, A. Sengupta, *Sens. Actuat. B* **129**, 909 (2008).
2. Andris Sutka, Rainer Parnab, Gundars Mezinskisa, Vambola Kisandb, *Sens. Actuat. B* **192**, 173 (2014).
3. N. Ponpandian, P. Balaya, A. Narayanasamy, *J. Phys.: Cond. Mater.* **14**, 3221 (2002).
4. C. Cheng, *Phys. Rev. B* **78**, 132403 (2008).
5. O.M. Hemeda, M.M. Barakat, *J. Magn. Magn. Mater.* **223**, 127 (2001).
6. S.C. Watawe, U.A. Bamne, S.P. Gonbare, R.B. Tangsali, *Mater. Chem. Phys.* **103**, 323 (2007).
7. M.M. Karanjkar, N.L. Tarwal, A.S. Vaigankar, P.S. Patil, *Ceramics Int.* **39**, 1757 (2013).
8. M. Muroi, R. Street, P.G. McCormick, J. Amighian, *Phys. Rev. B* **63**, 184414 (2001).
9. J. Wan, Y. Yao, G. Tang, *Appl. Phys. A* **89**, 529 (2007).
10. M.K. Randgolia, M.C. Chhandbar, A.R. Tanna, K.B. Modi, G.J. Baldha, H.H. Joshi, *Ind. J. Pure Appl. Phys.* **46**, 60 (2008).
11. M. Veith, M. Haas, V. Huch, *Chem. Mater.* **95**, 17 (2005).
12. A.J. Garcia-Adeva, D.L. Huber, *Phys. Rev. B* **65**, 184418 (2002).
13. V.S. Bushkova, B.K. Ostafiyuchuk, I.P. Yaremij, M.L. Mokhnatskyi, *Metallofiz. Noveishie Tekhnol.* **38**, 601 (2016).
14. S.K. Nath, K.H. Maria, S. Noor, S.S. Sikder, S.M. Hoque, M.A. Hakim, *J. Magn. Magn. Mater.* **324**, 2116 (2012).
15. S.H. Lee, S.J. Yoon, G.J. Lee, H.S. Kim, Ch.H. Yo, K. Ahn, D.H. Lee, K.H. Kim, *Mater. Chem. Phys.* **61**, 147 (1999).
16. B.H. Devmunde, A.V. Raut, S.D. Birajdar, S.J. Shukla, D.R. Shengule, K.M. Jadhav, *J. Nanopart.* **2016**, 4709687 (2016).
17. L.D. Tung, V. Kolesnichenko, D. Caruntu, N.H. Chou, C.J. O'Connor, L. Spinu, *J. Appl. Phys.* **93**, 7486 (2003).